Chalcogenide Letters Vol. 19, No. 11, November 2022, p. 847 - 854

$NiCo_2S_4$ nano composite structure with high electrochemical performance in band gap

V. Latha[a], K. Sambathkumar[b,*], N. Rajkamal[a], M. Venkatachalapthy[a]
[a]*Post Graduate and Research Department of Physics,Thiru.A.GovindasamyGovt Arts College, Tindivanam, Tamilnadu, India – 604002*
[b]*Post Graduate and Research Department of Physics, Ariginar.Anna.Govt.Arts College,Villupuram, Tamilnadu, India – 605602*

Synthesize $NiCo_2S_4$ and its application to find out electrochemical performance of anionic reaction in nano chemistry. Because of binary transition metal sulfide $NiCo_2S_4$ are prepared by using a Chemical precipitation to find out anionic movement within the compound. But the electrochemical were used as a conductive network for the $NiCo_2S_4$ hexagonal nano plates. Hence hexagonal nano plates have an average crystalline size of the particles 38.34nm and 20.06nm. Nickel and cobalt sulfides with various stoichiometries have been synthesized from Ni(CH3COO)2.2H2O, $CoCl_2.6H_2O$ with different sulfur precursors using as a direct method. The morphological composite were characterized by (scanning electron microscopy) SEM, XRD (X-ray diffraction), EDX, UV-visible, FTIR spectrum and optical band-gap energy were evaluated. Optical band-gap energies in the range 4.7 eV−5.1 eV were observed.

(Received August 2, 2022; Accepted November 22, 2022)

Keywords: SEM, FTIR, UV–Vis EDX, XRD, $NiCo_2S_4$

1. Introduction

Nickel and cobalt sulfides are good promising materials for researchers in the areas like solar cells, supercapacitors and electrode catalysts polymer materials. In storage conversion systems are extensively studied that are in practical applications in many fields, such as Lithium batteries, fuel storage cells and electrochemical capacitors. Batteries are long-term stability, fast charging, eco-friendly to the environment safety[1,2]. NiS, MnS, ZnS,CdS, CuS andCoS_2 [3-5]they can fulfill the gap between batteries and traditional storage capacitors. Recharge able batteries are associated with an electrode-potential-dependent accumulation of electrostatic charges with high power energy stability. $NiCo_2S_4$ having suitable pore size distribution are usually used as electrode materials as active carbon nano plates. Although many transition metal sulfides have been investigated as super capacitor electrode materials, reportson binary transition metal still limited[6-9].But irreversible volume change occurring during the intercalating process often leads to the high stability in electrochemical electrodes [10]. Metal-based materials can provide higher capacitance than conducting acids batteries. MnO_2, NiO_x, CoO_y, VO_z having more oxidation states, then electrode materials. Nickel sulfides and cobalt sulfides have been widely used in electrode materials due to their increase conductivity. The $NiCo_2S_4$ as the positive electrode and porous carbon as the negative electrode, exhibited excellent electrochemical reactions. Ni–Co binary oxides and binary sulfides may possess higher level electrochemical activity than nickel sulfides and cobalt sulfides based on redox active reactions. $NiCo_2S_4$ has higher conductivity and significant redox active properties of sulfides achieve higher power in rechargeable batteries[11,12]. $NiCo_2S_4$ with different shapes and good characters, such as a nano tubes, nano wires, hollow hexagonal nano plates, nano sheets, three-dimensional nano networks and cubic-like microstructures have been reported [13-16]. The synthesized $NiCo_2S_4$ with different morphologies

* Corresponding author: sa975kumar@gmail.com
https://doi.org/10.15251/CL.2022.1911.847

where modified for Chemical precipitation with an anion-ion exchange. The nano structured materials possess shorter diffusion distance, leading to a better electrochemical synthesis [17].

2. Experimental analysis

The phase composition and crystal structure of the prepared samples were characterized by X-ray powder diffraction (XRD) on a wide-angle X-ray diffractometer (Shimadzu XRD-6000/6100 model with 30kv, 30mA, Cu Ka radiation) with the 2q range from 10˚to 80˚. The surface morphology and microstructures of the products were examined by scanning electron microscope (SEM, XL30ESEM FEG).The composition of the products was explored by energy dispersion spectra (EDX) with a SEM attachment and elemental mapping images were performed. Existence of functional groups using the PerkinElmer spectrometer was verified via FTIR. With UV spectra were recorded on a Schimadzu UV-VIS-1601 spectrophotometer.

2.1. Synthesis of precursor serving as the templates

In this experiment, 0.476g of $CoCl_2.6H_2O$ (4mmol) and 0.249g of Ni(CH3COO)2.2H2O (2mmol) were dissolved in 40ml of deionized water to obtained a light pink solution, and then 3.2g of NaOH was added. After stirring for 10 min, the solution was transferred and then heated at 160^0c for 20hr. After cooling to room temperature naturally the gray precipitate was collected and washed again with deionized water several times and then dried at 60^0c for 5h. After precursor samples 0.093gas obtained and thenprecursorwasdispersedinto30mlofdeionizedwaterthrough magnetic stirrer. When 5mlof Na_2S solution was added in to the above suspension. And stirring for 5min, the suspension was transferred to oven for heat at 160^0c for 12h after cooled to room temperature naturally. Pale Black precipitate was obtained collected by filtration and washed with deionized water and then with ethanol for several times to remove the impurities. The resulting final product was dried in vacuum at 50^0c for 3h.And this chemical composition has influence on its electrochemical properties [18-20]. So as natural structure of honeybee structure is obtained for $NiCo_2S_4$ plays an important role in affecting the electrochemical process (Fig. 1).Redox-active reaction can take place not only on the lower surface area or surface region, but also in the bulk of active chemicals. The electrode is suitable for OH^-penetration, this further increases the utilization of active electrolyte. The active electrolyte alleviate strain stress and volume change during the charge and discharge of batteries processes especially under high loading current densities, which further ensure its durability.$NiCo_2S_4$ is directly in situ grown on a conductive Ni substrate without any binding chemicals. $NiCo_2S_4$ is a good conductivity comparable to other metals [21]but all the chemicals were purchased from Sigma Aldrich in analytical grade and were used without further purification.

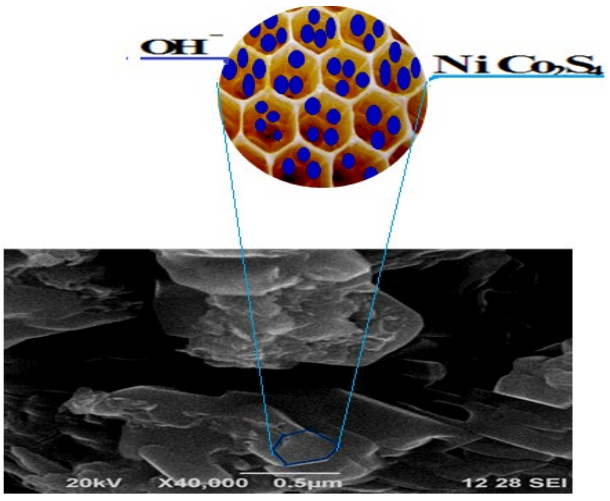

Fig. 1.Reaction of NiCo2S4 and OH⁻ in the electrochemical process.

3. Result and discussion

3.1. XRD Structural analysis

The structure of crystal phases were synthesized and investigated by the X– ray diffraction (XRD) analysis. The synthesized samples of XRD pattern are shown in Fig.2 (a-b).Fig.2 (a-b) shows a typical XRD Pattern of the precursor and$NiCo_2S_4$the diffraction peaks of which correspond to both (JCPDSNO:73-1297) have similar structure and very close diffraction peaks, it is difficult to differentiate these two of$NiCo_2S_4$ sample prepared by chemical precipitation method treating the precursor withNa_2S solution, which corresponds to spiral. The lattice parameters are estimated from the XRD single line position. The fine peaks appearing at 30.27°, 53.45° and 35.49° corresponds to lattice planes (111), (220) and (311) of cubic $NiCo_2S_4$ respectively. Two main peaks are observed at 30.27° and 35.49°, which are ascribed to the (111) and (311) planes, corresponding to the ternary phase of the nickel cobalt sulfide. But one strong peak was observed at 53.45° which is in good agreement with the $NiCo_2S_4$.The peak positions closely match JCPDS card 73-1297, with the synthesized composites exhibiting a cubic crystal structure with lattice parameters a = b = c = 7.93, which closely follows standard result. The standard diffraction peaks shown the crystal structure of precursor and$NiCo_2S_4$nano crystalline is hexagonal nano plate structure. The effect of precursor and$NiCo_2S_4$ on the structure change such as the lattice parameter and average crystalline size was studied at same observation. The crystalline single phase structure was described by the intense peaks. But the average crystallite size D was calculated using the Deby-Scherrer formula

$$D=\frac{0.9\lambda}{\beta cos\theta}$$

where, λ is the wavelength of x-ray used (1.5406 A^0), β is the full at half maximum in ration along (220) plane peaks of precursor and $NiCo_2S_4$nano crystalline hexagonal nano rods.

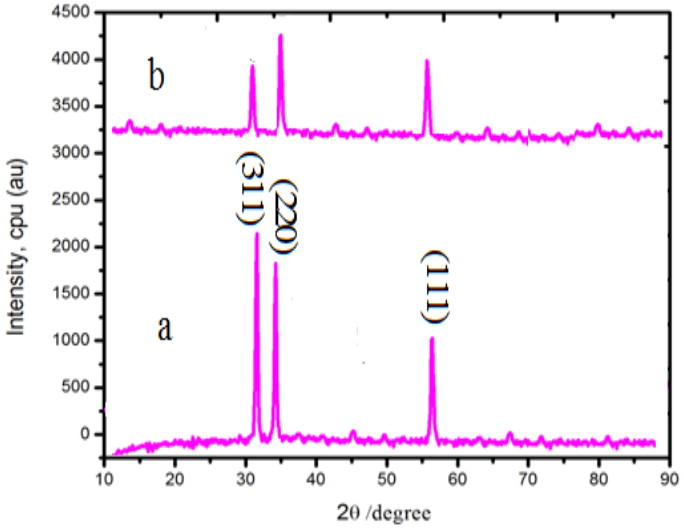

Fig. 2. XRD patterns of the $NiCo_2S_4$.

3.2. Surface morphology analysis (SEM/EDX)

SEM image is the precursor sample in which many uniform hollow hexagonal nano plates with an average diameter 0.5µm.SEM image display of the$NiCo_2S_4$sample prepared by treating the precursor in Na_2S as solution at 160°C for 12h. The $NiCo_2S_4$sample still retained the hexagonal nano plates morphology of the precursor, specifically a broken nano plates and sheets clearly reveals the hallow structure of the $NiCo_2S_4$. $NiCo_2S_4$ uniformly covered with different types of nanostructure, including more petal-shaped structures similar to the top view of a rose, spherical nano plates, and interconnected nano flakes [22,23]. It clearly observed that the nanostructure,

nano depth, nano thickness, and nano length of the vertical interconnected nano petals were affected by the ratio of Ni, Co to S. $NiCo_2S_4$ (Fig. 3(a,b)) exhibited an equal covering of larger-sized nano plates with porous structures. Vertically inter connected nano plates in a barrier-single wall-benzene structure (as shown in Fig. 3b). This type of nanostructure provides a large and wide active surface area and faster ion transfer during the electrochemical reaction within the $NiCo_2S_4$. The elemental composition of $NiCo_2S_4$ plate is given in the Tables 1 and 2 which confirm formation of a porous nanostructure. The EDX analysis confirmed the presence of precursor in $NiCo_2S_4$ System. Nearly and equal to their terminal stoichiometry with in the experimental error. Therefore the EDX spectra show well agreement with the experimental data concentration used for template directed synthesis of $NiCo_2S_4$ Figs 4.

Table 1.The quantitative of the composition element present for the precursor using EDX spectra.

Element	Intensity	Weight%	Atomic%
O	1.8523	35.77	69.05
Co	0.8098	44. 25	21.08
Ni	0.9533	19. 08	9.87

Table 2.The quantitative of the composition element present for the $NiCo_2S_4$ using EDX spectra.

Element	Intensity	Weight%	Atomic%
S	0.8795	25.88	39.06
Co	0.9040	49. 51	40.36
Ni	0.9837	24. 79	20.58

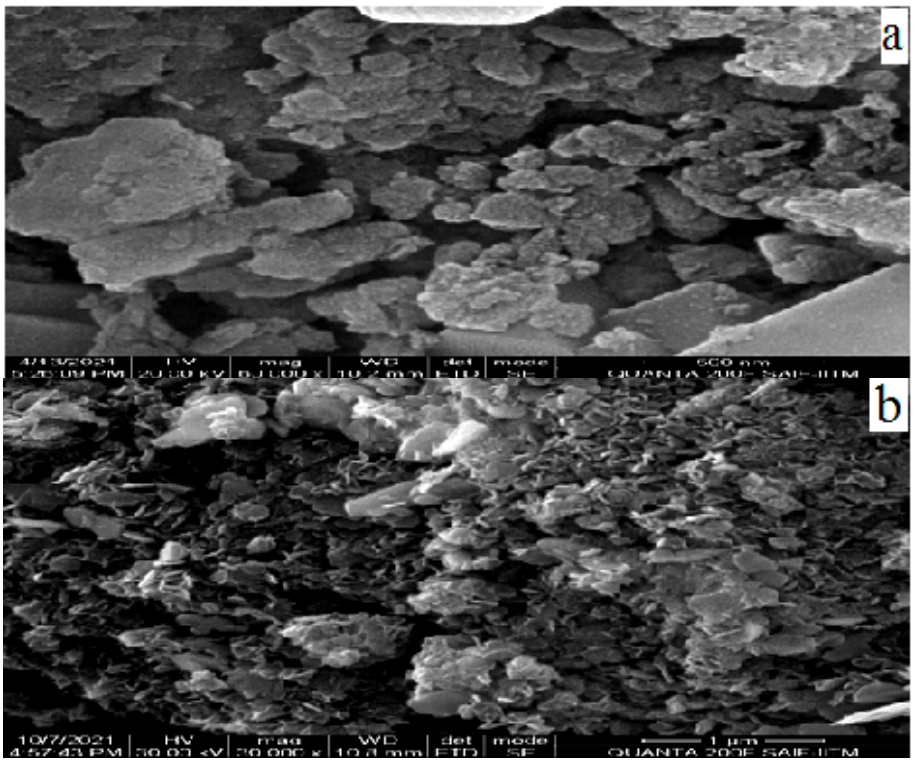

Fig. 3. SEM image of the $NiCo_2S_4$.

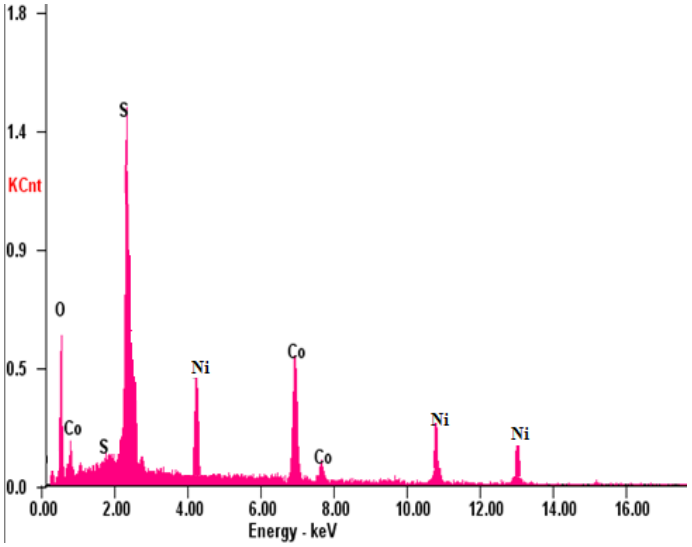

Fig.4. EDX spectrums of the $NiCo_2S_4$.

3.3. UV-visible study

UV-visible spectra analysis is a useful technique for the characterization of semiconductor nano particles,which exhibit quantum size effect caused by the photo generate electron hole pairs. The visible absorption spectra of semiconductor nano particles depends on their size and shape. The absorption maximum decrease with the nano particles size and shape Fig 5. (a-b) shows the UV-visible spectra of the composition of the precursor and $NiCo_2S_4$Sample were determined by UV-visible spectra. The absorption peaks were observed around 260 nm and 270 nm. These peaks are considerably blue-shifted compared to that of the bulk phase [23]. This absorption shift is due to quantum size effect representing a charge band gap along with excitation feature which can be used to measure the particles size and shape distribution. But optical band gaps increased with increasing particle sizes using sulfur materials. The calculated forbidden gap for these particles using composition of the precursor and $NiCo_2S_4$ indicates a direct electron transition between the states of the semiconductors. E_g = 5.1 eV and 4.5eV according to the formula of $E_g = (hc/\lambda)$eV is much larger than that of the bulk 4.0eV. It is shown infig.6 (a-b) that the absorption on set is blue shifted with decreasing value of $NiCo_2S_4$.which is an evidence of quantum mechanical effect.

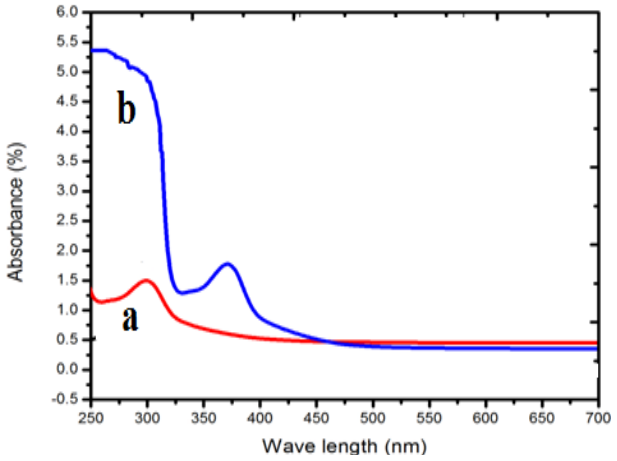

Fig. 5.UV-Visible spectrum of the$NiCo_2S_4$.

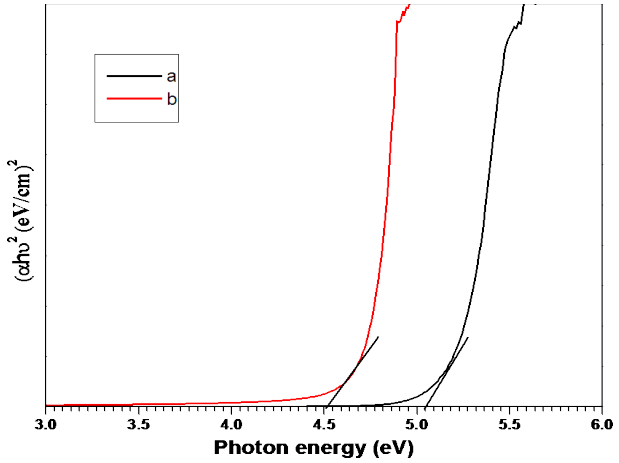

Fig. 6. Band gap energy of the$NiCo_2S_4$.

3.4. Functional group analysis(FTIR)

The presence of various chemical functional group and formation of precursor and $NiCo_2S_4$nanoplates are supported by FT-IR spectra as shown in fig 7(a-b).The broad absorption bands 3631 cm^{-1} and 3415 cm^{-1} are due O-H stretching and bending vibration of absorbed water at the surface of atoms. The absorption peak around2362 cm^{-1} is due to the existence of Co_2 molecules. The strong absorption bands between 560 cm^{-1} and 409 cm^{-1} can be attributed to the stretching mode of Ni, Co, S. Practically all these functional groups are the formation of cobalt sulfide nano particles using Na_2S.The appearance of the absorption band 409 cm^{-1} explains the morphology depending of the synthesized precursor of $NiCo_2S_4$nanoplates. The recorded peaks between1600cm^{-1}and1400cm^{-1}corresponds to the asymmetric and symmetric stretching of the carboxyl group(C=0).The peak around 670 cm^{-1} and 617 cm^{-1} corresponds to the bending vibration of precursor and $NiCo_2S_4$ hollow hexagonal nano plates. After heating, the peak of 670 cm^{-1} and 617 cm^{-1} is shown with very high intensity. The FTIR spectra also confirmed the stability of the prepared cobalt sulfide by the absence of any cobalt oxide [23]. Therefore Concentration with masses of attached atoms also influences the intensity and frequency of the peak. As the masses of attached atoms increase, wave number decreases and as concentration decreases, the intensity is also decreased for $NiCo_2S_4$ nanoplates.

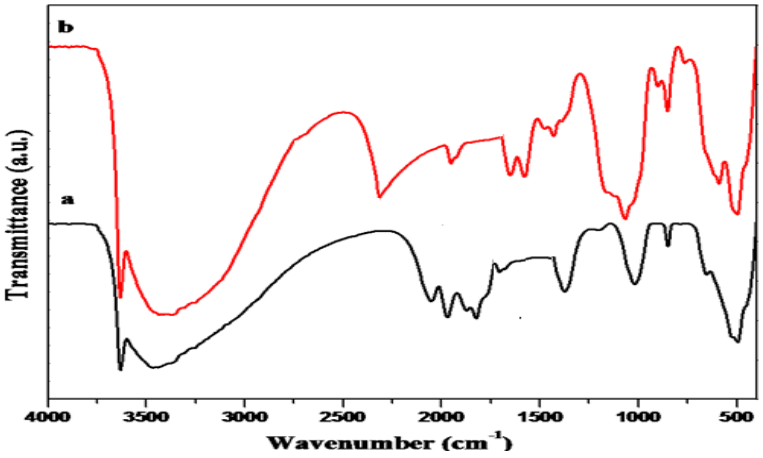

Fig. 7. FTIR spectrum of the $NiCo_2S_4$.

4. Conclusion

Synthesis and characterization of metal nano particles using chemical precipitation method. Ununiform grain size has been synthesized by simple chemical precipitation method. The calcinations temperature has a remarkable influence on the nucleation which leads to the formation of hexagonal nano plates structure. The estimated particle size by the XRD studies was found to be below 20 nm. The FTIR results show that the main band corresponding to the formation of $NiCo_2S_4$ appears around 670 cm^{-1}, this confirmed the samples. The energy gap by graphical determination has been 5.1 eV and 4.5eV. Moreover, the UV emission peak at 260 nm and 270 nm and the UV emission peaks blue shift to higher energy. The XRD, EDX and FTIR analysis implicate impurity of synthesized in $NiCo_2S_4$.

References

[1] Deng F, Tie J, Lan B, Sun M., Peng S, Deng S, Li B, Sun W, Yu L et al 2015 Electochimica. Acta. 176 359; https://doi.org/10.1016/j.electacta.2015.07.027

[2] Wang H, Wang C, Qing C, Sun D, Wang B, Qu G, Sun M, Tang Y et al 2015Electrochimica. Acta. 174 1104; https://doi.org/10.1016/j.electacta.2015.06.074

[3] PandiselviKannusamy and ThambiduraiSivalingam 2013 J. Poly. Degr .Stability. 98 988; https://doi.org/10.1016/j.polymdegradstab.2013.02.015

[4] TetsuroSoejima, Kohei Takada and Seishiro 2013 J. Appl Surf .Sci. 277 192; https://doi.org/10.1016/j.apsusc.2013.04.024

[5] Wu J B, Li Z G, Huang X H and Lin Y 2013 J. Power. Sources. 224 1; https://doi.org/10.1016/j.jpowsour.2012.09.085

[6] Li Y, Cao D, Wang Y, Yang S, Zhang D, Ye K, Cheng K, Yin J, Wang G, Xu Y et al 2015 J. Power .Sources. 279 138; https://doi.org/10.1016/j.jpowsour.2014.12.153

[7] Zhu Y, Ji X, Wu Z and Liu Y 2015 Electrochimica. Acta. 186 562; https://doi.org/10.1016/j.electacta.2015.10.176

[8] Wu Z, Pu X, Ji X, Zhu Y, Jing M, Chen Q, Jiao F et al 2015 Electrochimica. Acta. 174 238; https://doi.org/10.1016/j.electacta.2015.06.011

[9] Liang J, Xi K, Tan G, Chen S, Zhao T, Coxon P R, Kim H, Ding S, Yang Y, Kumar R.V, Lu J et al 2016 Nano. Energy. 27 457; https://doi.org/10.1016/j.nanoen.2016.06.032

[10] Yu M. Chen J, Ma Y, Zhang J, Liu J, Li S, An J et al 2014 Appl. Surf. Scie. 314 1000; https://doi.org/10.1016/j.apsusc.2014.06.125

[11] Tang Y, Chen S, Mu S, Chen T, Qiao Y, Yu S, Gao F et al 2016 ACS. Appl. Mate. Interf. 8 9721; https://doi.org/10.1021/acsami.6b01268

[12] Xiao Y, Su D, Wang X, Zhou L, Wu S, Li F, Fang S et al 2015 Electrochimica. Acta. 176 44; https://doi.org/10.1016/j.electacta.2015.06.128

[13] Chu Q, Wang W, Wang X, Yang B Liu X and Chen J 2015 J. Power. Sources. 276 19; https://doi.org/10.1016/j.jpowsour.2014.11.015

[14] Jin R, Liu D, Liu C and Liu G 2015 RSC. Advances. 5 84711; https://doi.org/10.1039/C5RA14412D

[15] Zou R, Zhang Z, Yuen M F, Sun M, Hu J, Lee C.-S, Zhang W et al 2015 NPG. Asia .Mater. 7 195; https://doi.org/10.1038/am.2015.63

[16] Zeng Z, Wang D, Zhu J, Xiao F, Li Y, Zhu X et al 2016 Cryst .Eng .Comm. 18 2363; https://doi.org/10.1039/C6CE00319B

[17] Li R, Wang S, Huang Z, Lu F and He T 2016 J. Power. Sources. 312 156; https://doi.org/10.1016/j.jpowsour.2016.02.047

[18] Yang B, Yu L, Yan H, Sun Y, Liu Q, Liu J, Song D, Hu S, Yuan Y, Liu L J, Wang et al 2015 J of Materials Chemistry A 3 13308.

[19] Niu H, Zhou D, Yang X, Li X, Wang Q, Qu F et al 2015 J Mater. Chemistry. A 3 18413;

https://doi.org/10.1039/C5TA04311E
[20] Xiao J, Zeng X, Chen W, Xiao F and Wang S 2013 Chemical. Communications. 49 11734; https://doi.org/10.1039/c3cc44242j
[21] Xia C, Li P, Gandi A N, Schwingenschlögl U and Alshareef H N 2015 Chemistry. Mater. 27 6482; https://doi.org/10.1021/acs.chemmater.5b01843
[22] Shinde S K, Sivalingam Ramesh, Bathula C, Ghodake G S, Kim D-Y, Jagadale A D, Kadam A A, Waghmode D P, Sreekanth T V. M, Heung Soo Kim, nagajyothi P C, Yadav H M et al 2019 Scientific. Reports. 9 13717; https://doi.org/10.1038/s41598-019-50165-5
[23] Aboelazm, E A A 2018 J..Phys. ChemC. 122 12200; https://doi.org/10.1021/acs.jpcc.8b03306